

**High-order harmonics from an ultraintense laser pulse propagating inside a fiber**S. V. Bulanov,<sup>1,\*</sup> T. Zh. Esirkepov,<sup>2,†</sup> N. M. Naumova,<sup>1,3,‡</sup> and I. V. Sokolov<sup>4,§</sup><sup>1</sup>General Physics Institute RAS, Vavilov Street 38, Moscow 119991, Russia<sup>2</sup>Moscow Institute of Physics and Technology, Institutskij per. 9, Dolgoprudny Moscow region 141700, Russia<sup>3</sup>Center for Ultrafast Optical Science, University of Michigan, 2200 Bonisteel Boulevard, Ann Arbor, Michigan 48109-2099<sup>4</sup>Space Physics Research Laboratory, University of Michigan, 2455 Hayward Avenue, Ann Arbor, Michigan 48109-2143

(Received 22 May 2002; published 28 January 2003)

A strong effect of high harmonic radiation during the propagation of a high intensity short laser pulse in a thin wall hollow channel (“fiber”) is found and studied via relativistic particle-in-cell simulations. The fiber has finite width walls comprised of an overdense plasma. Only the harmonic radiation with the harmonic number above critical value, for which the fiber walls are transparent, propagates outwards in the form of a coherent ultrashort pulse with very short wavelength.

DOI: 10.1103/PhysRevE.67.016405

PACS number(s): 42.65.Ky, 52.25.Os, 52.65.Rr, 52.27.Ny

**I. INTRODUCTION**

The generation of high-order harmonics of the electromagnetic radiation during the interaction of high-intensity laser pulses with underdense and overdense plasmas is a manifestation of one of the most basic nonlinear processes in physics. High-order optical harmonics have been observed in the laser interaction with plasmas for the radiation intensity ranging from moderate level to relativistic intensities.

High-order harmonics attract great attention due to a wide range of their applications for the diagnostics, the UV and x-ray sources of coherent radiation, lithography, etc. (see Refs. [1–5]). Recently, the polarization properties of high-order harmonics have been used in Ref. [6] to detect the highest strength magnetic field generated in the laser plasmas.

The physical mechanisms of the generation of high-order harmonics have much in common because they are based on a property of nonlinear systems to react in an anharmonic manner on the action of a periodic driving force. On the other hand, a specific realization of this property depends on the circumstances of the laser-matter interaction and mainly on the laser intensity. At the moderate intensity, the generation of high-order harmonics occurs due to the anharmonicity of the atom response on the finite amplitude oscillating electric field. When the laser radiation intensity becomes above the level where the electron quiver energy is higher than the rest mass energy and the *relativistic nonlinear optics* comes into play [4], the generation of high order harmonics is due to nonlinear dependence of the particle mass on the momentum and due to modulations of the electron density in the electromagnetic wave.

Further in the present paper we shall address the high harmonic generation in collisionless plasmas in the limit of relativistically strong electromagnetic wave.

In the underdense plasmas the high harmonics are produced by the mechanism of the parametric excitation of the electromagnetic and electrostatic waves with different frequencies. When the laser radiation interacts with the overdense plasmas, it reflects back at the plasma-vacuum interface in the case of the sharp plasma boundary, or at the surface of critical density, in the case of the gradual density profile. The reflection layer of the plasma dragged by the electromagnetic wave back and forth as well as in the plane of the surface of the plasma-vacuum interface (in the plane of the critical surface) forms the oscillating mirror (see Refs. [7–13]). The spectrum of the light reflected at the oscillating mirror contains odd and even harmonics, whose polarization and amplitudes depend on the incidence angle of the pulse, its intensity and the pulse polarization.

High efficiency of the laser energy transformation into the energy of the high harmonic radiation can be achieved when the laser pulse propagates inside a hollow plasma channel [14]. In this case, if the channel is sufficiently long, we actually have multiple reflections of the laser pulse at the vacuum-plasma interface with a transformation of a portion of the laser energy into high harmonics at each reflection event. If the laser pulse interacts with a fiber, i.e., when it propagates inside a hollow, thin wall channel, in addition, it becomes possible to extract the high frequency radiation from the fiber. We assume that the fiber walls are transparent for harmonics whose indices are above some critical value. Only these harmonics propagate outwards, at a certain angle with respect to the fiber axis. This scheme provides an approach to make the high frequency radiation source with controlled properties, changing the fiber diameter and the wall thickness.

In the present paper we study the propagation of a high intensity short laser pulse in a fiber, with the aim to study the properties of the high harmonic radiation. We use the two dimension approximation leaving the investigation of the 3D problem for forthcoming publications.

**II. MATCHING CONDITIONS**

In the two-dimensional case the fiber corresponds to the configuration made by two finite length thin layers parallel to the  $x$  axis in the  $(x,y)$  plane. The thickness of the layer is  $l$

\*Also at Advanced Photon Research Center, JAERI, Kizunani, Kyoto-fu 619-0215, Japan. Electronic address: bulanov@apr.jaeri.go.jp

†Electronic address: timur@nonlin.mipt.ru

‡Electronic address: naumova@engin.umich.edu

§Electronic address: igorsok@umich.edu

with a distance between the layers equal to  $L$ . We consider the layers comprised the collisionless overdense plasma with the electron density  $n_e$ . Such a configuration can be formed during interaction of the high intensity femtosecond laser pulse with the solid density fiber walls when the wall material is ionized during the first half period of the laser pulse, and the length of the laser pulse is much shorter than the time of the hydrodynamic expansion of the plasma. In this case the plasma layer on the fiber wall can be considered as a cladding. Within the framework of this approximation we can assume the ions in the plasma layer to be at rest.

From the dispersion equation,  $\omega^2 = k^2 c^2$ , where  $\omega$  is the wave frequency and  $k^2 = k_x^2 + k_y^2$ , we find the group velocity of the wave inside the channel to be equal to  $v_{gr} = \partial\omega/\partial k_x = (c/\omega)(\omega^2 - \pi^2/L^2)^{1/2} = c \cos \theta$ , where  $\tan \theta = k_y/k_x = (4L^2/\lambda^2 - 1)^{-1/2}$  and  $\lambda = 2\pi c/\omega$ . The matching conditions for the waves inside the channel and the waves radiated outwards show that the waves radiated outwards propagate at the angle  $\theta$  with respect to the channel axis, irrespective of the wave frequency.

The fact that all the outgoing waves have the same angle of propagation can be demonstrated in a different way. After the Lorentz transformation into the reference frame moving at a speed equal to the laser pulse group velocity  $v_{gr}$  along the  $x$  direction, the  $x$  component of the wave vector vanishes  $k'_x = 0$  (see for details Refs. [7,10,15]). In the moving reference frame the problem becomes one-dimensional. We see that the high frequency waves excited by the fundamental mode at the plasma-boundary interface also have in this frame the zero  $x$  component of the wave vector, i.e., propagate outwards in the normal direction to the channel walls irrespective of the wave frequency. Performing the Lorentz transformation into the laboratory frame, we find that the waves radiated outwards propagate at the same angle  $\theta$  with respect to the channel axis. Their energy is localized inside a slab comoving with the laser pulse along the  $x$  axis. The transverse size of the slab depends on the effective length of the interaction. According to the selection rules of the harmonic generation at each wall (see Refs. [7,9,10]), the  $s$ -polarized fundamental mode generates  $s$ -polarized odd harmonics and  $p$ -polarized even harmonics. The  $p$ -polarized fundamental mode generates only  $p$ -polarized odd and even harmonics.

The amplitude of the  $n$ th harmonic wave can be found in the framework of the approximation of a thin layer for the channel walls (see Ref. [10]). It is  $E^{(n)} = K^{(0,n)} E^{(0)}$ , where  $E^{(0)}$  and  $E^{(n)}$  are amplitudes of the fundamental mode and of the  $n$ th harmonic, respectively. The transformation coefficient  $K^{(0,n)}$  in the limit  $n\omega/\omega_{pe} \ll \varepsilon$  is given by  $K^{(0,n)} \approx [(a_0/\varepsilon) \sin \theta]^n$ . Here  $a_0 = eE^{(0)}/m_e \omega_0 c$  is the dimensionless amplitude of the fundamental mode,  $\varepsilon = 2\pi n_0 e^2 l / m_e \omega_0 c$  is the dimensionless parameter and  $\omega_0$  is the frequency of the fundamental mode. The parameter  $\varepsilon$  is the relativistic transparency measure as it is discussed in Ref. [3].

### III. PARAMETERS OF COMPUTER SIMULATIONS

We perform computer simulations using the two-dimensional version of particle-in-cell electromagnetic rela-

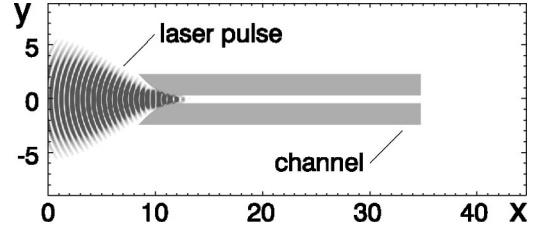


FIG. 1. The electromagnetic energy density and the plasma density distribution at  $t = 15 \times 2\pi/\omega_0$  when the pulse enters the fiber. The space coordinates are measured in the laser wavelengths.

tivistic code REMP, based on the “density decomposition” scheme (see Ref. [16]). The computation box has the size  $45\lambda \times 20\lambda$ . Since the problem of high harmonic generation requires a sufficiently high spatial resolution, the computation mesh has 50 cells per  $\lambda$ . The particle number per cell is equal to 16 in the plasma region. The channel walls have a length  $l_{ch} = 25\lambda$  and width  $2\lambda$  with a distance between the walls  $L = 0.7\lambda$ . The ions are assumed to be immobile and the electron density is equal to  $8n_{cr}$ , where the critical density is  $n_{cr} = \omega_0^2 m_e / 4\pi e^2$ . Since the channel is assumed to have the distance between the walls less than the laser light wavelength, only the  $s$ -polarized electromagnetic wave, whose electric field is directed along the  $z$  axis, can propagate inside the channel. For the parameters chosen, only the high harmonics whose index is higher than 4 can penetrate the walls. This condition follows from the boundary conditions for the electromagnetic wave at the plasma-vacuum interface for the oblique incidence at the angle  $\theta$ . The  $s$ -polarized laser has been initialized in a vacuum region at the left-hand side from the channel entry. The pulse aperture is  $f/1$ , the length is equal to  $7.5\lambda$  and the dimensionless amplitude at the  $1\lambda$  focus spot is  $a_0 = 3$ , which corresponds to the intensity  $I \approx 10^{19}$  W/cm<sup>2</sup>. These parameters correspond to the parameters of the laser in the CUOS at the University of Michigan [4]. We notice here that the pulse focusing into the  $1\lambda$  focus spot has been discussed in Ref. [4]. In our simulation model the entry of the channel has been smoothed to decrease the laser pulse reflection here. Figure 1 illustrates the laser pulse–fiber configuration. It shows the focusing of the laser pulse on the channel entry. We see that the smoothing of the channel entry provides almost reflectionless matching of the laser pulse and the channel.

### IV. RESULTS OF 2D PIC SIMULATIONS

When the laser pulse propagates inside the channel, a portion of its energy is reflected back due to the process similar to the stimulated Raman scattering in the plasma of the channel walls; a portion of its energy is transformed into the energy of high harmonic waves radiated outwards; the remaining part of the laser pulse propagates through the channel toward the end of the channel; then at the right-hand side vacuum region it forms the diverging electromagnetic wave. These successive processes are seen in Fig. 2, where we present the electromagnetic energy density distribution in the  $(x, y)$  plane at  $t = 20 \times 2\pi/\omega$  in frame (a), at  $t = 35 \times 2\pi/\omega$  in frame (b), and at  $t = 50 \times 2\pi/\omega$  in frame (c).

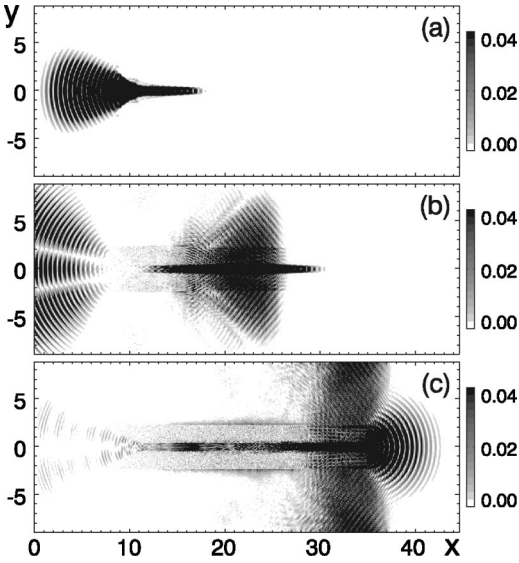


FIG. 2. The electromagnetic energy density distribution in the  $(x, y)$  plane at  $t = 20 \times 2\pi/\omega$  in frame (a), at  $t = 35 \times 2\pi/\omega$  in frame (b), and at  $t = 50 \times 2\pi/\omega$  in frame (c). The space coordinates are measured in the laser wavelengths.

In Fig. 3 we show the distribution of the  $z$  component of the electric field in the  $(x, y)$  plane at  $t = 45 \times 2\pi/\omega_0$ . This figure provides the visualization of odd-index high harmonics, which have the  $s$  polarization, as noticed above. We see the laser pulse inside the channel and the high harmonics aside the channel. The spacial region filled by high harmonics has a length along the  $x$  axis equal to the laser pulse length and the transverse size (along the  $y$  axis) equal to  $\delta t c \sin \theta$ , where  $\sin \theta \approx 1/2$  and  $\delta t \approx 20 \times 2\pi/\omega_0$ .

We performed the spatial Fourier transformation of the  $z$  component of the electric field inside a subdomain ( $25\lambda < x < 35\lambda$ ;  $3\lambda < y < 10\lambda$ ) at  $t = 45 \times 2\pi/\omega_0$ . The resulting spectrum of the  $s$ -polarized light inside this subdomain is presented in Fig. 4. We see the odd-number harmonics with the harmonic index  $n = (k_x^2 + k_y^2)^{1/2} \leq 5$ . The spectrum peaks in the  $(k_x, k_y)$  plane are arranged along the straight line given by expression  $k_y \approx 0.8k_x$ , i.e., the propagation angle is smaller than  $\arccos(1 - \pi^2 c^2/\omega_0^2 L^2)^{1/2}$ . This means that the actual channel width is larger than  $0.7\lambda$ . The increase of the channel width apparently is due to the action of the ponderomotive force on the electrons at the vacuum-plasma interface. From the expression  $m_e c^2 \nabla(1 + a^2)^{1/2} \approx 4\pi n_0 e^2 \delta y$ , which corresponds to the balance between the ponderomotive force and the force that acts on the electrons in the

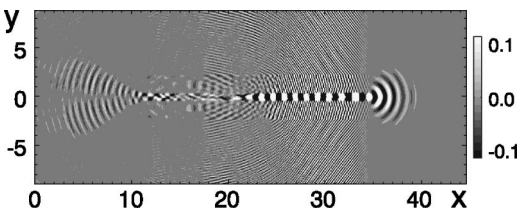


FIG. 3. Distribution of the  $z$  component of the electric field in the  $(x, y)$  plane at  $t = 45 \times 2\pi/\omega_0$ . The space coordinates are measured in the laser wavelengths.

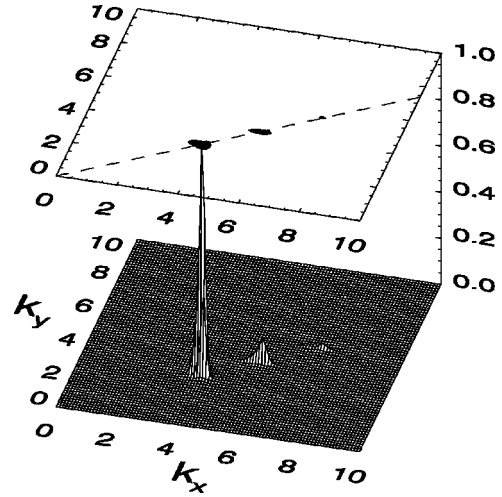


FIG. 4. Spectrum of the  $s$ -polarized light in the  $(k_x, k_y)$  plane calculated inside the subdomain  $25\lambda < x < 35\lambda$ ;  $3\lambda < y < 10\lambda$  at  $t = 45 \times 2\pi/\omega_0$ . The wave-vector components are measured in the  $2\pi/\lambda$  units. Dashed line corresponds to the dependence  $k_y \approx 0.75k_x$ .

electric field of the electric charge separation, we find that the channel width becomes larger on  $2\delta y \approx 0.1\lambda$ . In the case of the channel width equal to  $0.8\lambda$  the propagation angle is  $\theta_{eff} \approx \arctan(0.8) \approx 38^\circ$  in agreement with the dependence seen in Fig. 4.

In Fig. 5 we present the distribution of the  $z$  component of the magnetic field in the  $(x, y)$  plane at the same instant of time as Fig. 4 ( $t = 45 \times 2\pi/\omega_0$ ). We see the even high harmonics. They are  $p$  polarized. As noticed above, the fundamental mode of the laser pulse inside the channel does not contain the  $p$ -polarized component and we see only the high harmonics inside and aside the channel, as well as the low frequency surface mode in the vicinity of the outer vacuum-plasma interfaces on both sides of the channel. The even-index high harmonics outside the channel are localized in the same region as the odd-index harmonics.

The spectrum of the even high harmonics calculated for the field inside the same sub-domain as in the case of the odd harmonics is presented in Fig. 6. We see the even harmonics with the harmonic index  $n \leq 6$ . As in the previous figure, the spectrum peaks are also arranged in the  $(k_x, k_y)$  plane along the straight line given by expression  $k_y \approx 0.8k_x$ .

V. CONCLUSION

Via particle-in-cell simulations we demonstrated the high harmonic generation during the interaction of the relativisti-

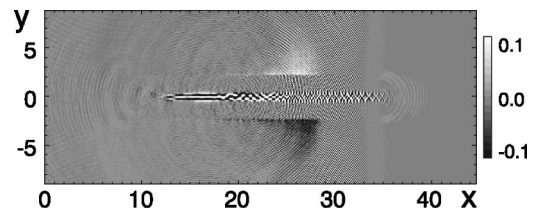


FIG. 5. Distribution of the  $z$  component of the magnetic field in the  $(x, y)$  plane at  $t = 45 \times 2\pi/\omega_0$ . The space coordinates are measured in the laser wavelengths.

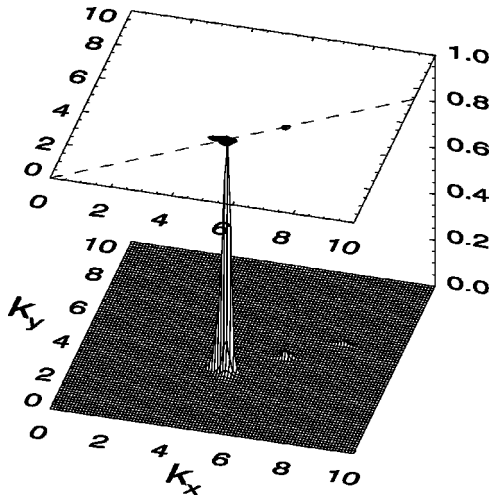


FIG. 6. Spectrum of the  $p$ -polarized light in the  $(k_x, k_y)$  plane calculated inside the subdomain  $25\lambda < x < 35\lambda$ ;  $3\lambda < y < 10\lambda$  at  $t = 45 \times 2\pi/\omega_0$ . The wave-vector components are measured in the  $2\pi/\lambda$  units. Dashed line corresponds to the dependence  $k_y \approx 0.75k_x$ .

cally intense short laser pulse with a narrow fiber. Due to the nonlinear interaction of the laser pulse with the fiber walls, the electrons quivering back and forth form the oscillating mirrors. The high-order harmonics are generated as a result

of a multiple reflection of the laser light from the oscillating mirrors. The fiber walls are nontransparent for the electromagnetic wave with a frequency below critical value, which depends on the electron density inside the walls and the channel width. As a result, only the harmonic radiation with a sufficiently high harmonic index, for which the fiber walls are transparent, propagates outwards at a certain angle, irrespective of the harmonic index. In addition, we observe in the  $p$ -polarized wave the low frequency mode excitation, which is localized at the outer surface of the fiber. The longitudinal scale of the low frequency mode is of the order of the laser pulse length. It provides an example of the nonlinear rectification of the light. The high harmonic energy is localized in the region with a length (along the  $x$  direction) being equal to the laser pulse length, and the width (along the  $y$  direction) being equal to  $l_{ch} \tan \theta_{eff}$ . The high harmonic pulse comoves along the  $x$  axis with the laser pulse inside the channel. The amplitude of the  $n$ th harmonic can be estimated as  $(a_0 \sin \theta_{eff})^n (\omega_0/\omega_{pe})^{1+2n}$ , where  $\omega_{pe} = (4\pi n_0 e^2/m_e)^{1/2}$ . For  $a_0 = 3$ ,  $(\omega_0/\omega_{pe})^2 = 1/8$  and  $\theta_{eff} \approx 38^\circ$  we obtain  $E^{(n)}/E^{(0)} \approx 0.35(0.23)^n$ . This proves an effective mechanism for the generation of ultrashort pulses of coherent light with very short wavelengths.

#### ACKNOWLEDGMENTS

We thank Professor Y. Kato for fruitful discussion. This work is supported by INTAS Grant No. 001-0233.

- [1] N. Bloembergen, *Nonlinear Optics* (Addison-Wesley, Reading, MA, 1965); Y.R. Shen, *The Principles of Nonlinear Optics* (Wiley, New York, 1984); S.A. Akhmanov and R.V. Khokhlov, *Problems of Nonlinear Optics* (VINITI, Moscow, 1965); R.W. Boyd, *Nonlinear Optics* (Academic, San Diego, 1992).
- [2] J. Zhou, J. Peatross, M.M. Murnane, H.C. Kapteyn, and I.P. Christov, *Phys. Rev. Lett.* **76**, 752 (1996); Y. Kobayashi, T. Sekikawa, Y. Nabekawa, and S. Watanabe, *Opt. Lett.* **23**, 64 (1998); P. Villoresi *et al.*, *Phys. Rev. Lett.* **85**, 2494 (2000); C. Altucci *et al.*, *Phys. Rev. A* **61**, 021801(R) (1999).
- [3] S.V. Bulanov, F. Califano, G.I. Dudnikova, T.Zh. Esirkepov, I.N. Inovenkov, F.F. Kamenets, T.V. Liseikina, M. Lontano, K. Mima, N.M. Naumova, K. Nishihara, F. Pegoraro, H. Ruhl, A.S. Sakharov, Y. Sentoku, V.A. Vshivkov, and V.V. Zhakhovskii, in *Reviews of Plasma Physics*, edited by V.D. Shafranov (Kluwer Academic/Plenum, New York, 2001), Vol. 22, p. 227.
- [4] G. Mourou, Z. Chang, A. Maksimchuk, J. Nees, S.V. Bulanov, V.Yu. Bychenkov, T.Zh. Esirkepov, N.M. Naumova, F. Pegoraro, and H. Ruhl, *Plasma Phys. Rep.* **28**, 12 (2002).
- [5] P.A. Norreys, M. Zepf, S. Moustazis, A.P. Fews, J. Zhang, P. Lee, M. Bakarezos, C.N. Danson, A. Dyson, P. Gibbon, P. Loukakos, D. Neely, D.F.N. Walsh, J.S. Wark, and A.E. Dangor, *Phys. Rev. Lett.* **76**, 1832 (1996).
- [6] M. Tatarakis, I. Watts, F.N. Beg, E.L. Clark, A.E. Dangor, A. Gopal, M.G. Hains, P.A. Norreys, U. Wagner, M.-S. Wei, M. Zepf, and K. Krushelnik, *Nature (London)* **415**, 280 (2002); M. Tatarakis, A. Gopal, I. Watts, F.N. Beg, A.E. Dangor, K. Krushelnik, U. Wagner, P.A. Norreys, E.L. Clark, M. Zepf, and R.G. Evans, *Phys. Plasmas* **9**, 2244 (2002).
- [7] S.V. Bulanov, N.M. Naumova, and F. Pegoraro, *Phys. Plasmas* **1**, 745 (1994).
- [8] P. Gibbon, *Phys. Rev. Lett.* **76**, 50 (1996).
- [9] R. Lichters, J. Meyer-ter-Vehn, and A.M. Pukhov, *Phys. Plasmas* **3**, 3425 (1996).
- [10] A.V. Vshivkov, N.M. Naumova, F. Pegoraro, and S.V. Bulanov, *Phys. Plasmas* **5**, 2752 (1998).
- [11] A. Macchi, F. Cornolti, F. Pegoraro, T.V. Liseikina, H. Ruhl, and V.A. Vshivkov, *Phys. Rev. Lett.* **87**, 205004 (2001); A. Macchi, F. Cornolti, and F. Pegoraro, *Phys. Plasmas* **9**, 1704 (2002).
- [12] M. Zepf, G.D. Tsakiris, G. Pretzler, I. Watts, D.M. Chambers, P.A. Norreys, U. Andiel, A.E. Dangor, K. Eidmann, C. Gahn, A. Machacek, J.S. Wark, and K. Witte, *Phys. Rev. E* **58**, 5253 (1998).
- [13] J. Tarasevitch, A. Orisch, D. von der Linde, P. Balcou, G. Rey, J.-P. Chambaret, U. Teubner, D. Klöpffel, and W. Theobald, *Phys. Rev. E* **62**, 023816-1 (2000).
- [14] S.V. Bulanov, F.F. Kamenets, A.M. Pukhov, and F. Pegoraro, *Phys. Lett. A* **195**, 84 (1994).
- [15] A. Bourdier, *Phys. Fluids* **26**, 1804 (1983).
- [16] T.Zh. Esirkepov, *Comput. Phys. Commun.* **135**, 144 (2001).